nature catalysis

Article

https://doi.org/10.1038/s41929-025-01418-2

Enantioselective radical dearomative conjugate amination enabled by Co(II)-based metalloradical catalysis

Received: 25 November 2024

Accepted: 2 September 2025

Published online: 6 October 2025

Check for updates

Pan Xu [1,2], Duo-Sheng Wang [1], Zhenyu Zhu[1] & X. Peter Zhang [1]

Delocalized radical systems present a challenging yet appealing ground to test the control of multiple selectivity in organic synthesis. Despite some recent advances, the issue of regioselectivity in delocalized radical systems has largely centred on allylic radicals. To explore larger delocalized radical systems, we report the catalytic generation of extensively delocalized 4-vinylphenoxyl radicals and their involvement as key intermediates in regioselective radical C–N bond formation. Guided by the mechanistic principles of metalloradical catalysis, we develop a Co(II)-based enantioselective radical system for dearomative 1,7-conjugate amination of readily available 4-vinylphenols with aryl azides. This can afford valuable chiral α-tertiary amino acid derivatives in high yields with excellent enantioselectivities for the newly created tetrasubstituted stereocentres. Unlike previous systems, this amination involves hydrogen-atom abstraction from O–H bonds. As demonstrated with 1,6-conjugate addition with various nucleophiles, the resulting α-tertiary amino acid derivatives, which bear additional *para*-quinone methide functionality, may find useful synthetic applications.

The past decade has witnessed considerable growth in the development of new synthetic methods involving organic radicals as intermediates[1]. While manifesting the rich fundamental reactivity and attractive practical attributes of radical chemistry, this burgeoning exploration has also highlighted the long-standing challenges of controlling the reactivity and selectivity of radical reactions[2]. Among the diverse radical intermediates, delocalized radical systems pose an added challenge with the control of regioselectivity, alongside chemoselectivity and stereoselectivity, while presenting exceptional opportunities for constructing complex molecular structures. Among advances in catalytic strategies[3–11], metalloradical catalysis (MRC) has emerged as a general approach for controlling the reactivity and selectivity of homolytic radical reactions[12]. MRC exploits metal-centred radicals in open-shell metal complexes as one-electron catalysts for homolytic activation of substrates to generate metal-entangled organic radicals as the key intermediates to govern the reaction pathway and the stereochemical course of subsequent radical processes[13–31]. To this end, Co(II) complexes of porphyrins, which represent a family of stable 15-electron metalloradicals with a well-defined low-spin d^7 configuration, have demonstrated remarkable ability for homolytic activation of organic azides to generate α-Co(III)-aminyl radicals that can serve as competent intermediates for catalytic C–H amination[32,33]. With modularly designed D_2-symmetric chiral amidoporphyrins (D_2-Por*) as a versatile ligand platform[34], Co(II)-based MRC has been successfully applied for the development of an asymmetric radical process that can catalyse direct allylic C–H amination of 1,2-disubstituted alkenes with aryl azides[32]. This process involves intermolecular hydrogen-atom abstraction (HAA) from allylic C–H bonds by the initially generated α-Co(III)-aminyl radicals, followed by radical substitution directly at the original allylic site (Fig. 1a). As a further application of Co(II)-MRC for controlling regioselectivity, we have recently achieved asymmetric radical 1,3-conjugate allylic C–H amination of trisubstituted alkenes

[1]Department of Chemistry, Merkert Chemistry Center, Boston College, Chestnut Hill, MA, USA. [2]School of Chemistry and Chemical Engineering, Southeast University, Nanjing, China. e-mail: peter.zhang@bc.edu

https://doi.org/10.1038/s41929-025-01418-2

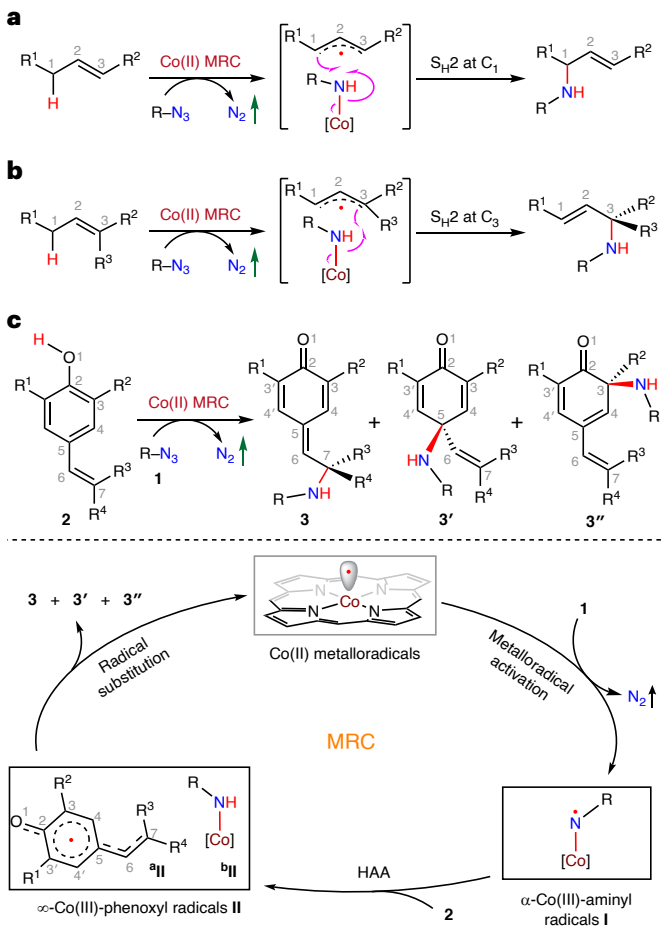

Fig. 1 | Regioselectivity in intermolecular radical amination processes involving delocalized radical intermediates. a, Direct C–H amination via delocalized allylic radicals (previous work). **b**, 1,3-Conjugate C–H amination via delocalized allylic radicals (previous work). **c**, Conjugate amination via delocalized 4-vinylphenoxyl radicals (this work).

with aryl azides, with concurrent control of diastereoselectivity and enantioselectivity (Fig. 1b)[33]. The key to this success lies in effective catalyst design through tailored ligand engineering, creating an optimal catalytic environment that maximizes the desired non-covalent attractive interactions in key intermediates to govern regioselectivity between direct and 1,3-conjugate allylic C–H amination. Prompted by these recent findings, we wondered whether Co(II) MRC could be explored to control regioselectivity, in addition to chemoselectivity and stereoselectivity, in a larger and more extensively delocalized radical system than allylic radicals.

Among large delocalized radical systems, we were particularly intrigued by the possibility of catalytic amination of 4-vinylphenols with organic azides via Co(II) MRC, which may involve 4-vinylphenoxyl radical intermediates. This class of oxygen radicals is known for extensive spin delocalization in their π-conjugate system (Fig. 1c). Given that the bond dissociation energy of phenolic O–H bonds (~87 kcal mol^{-1}) is similar to that of benzylic C–H bonds (~90 kcal mol^{-1}) and allylic C–H bonds (~89 kcal mol^{-1}), we hypothesized that the initially generated α-Co(III)-aminyl radical **I** from metalloradical activation of organic azide **1** could engage HAA from the O–H bond in vinylphenol **2**. This would generate ∞-Co(III)-amido phenoxyl radical intermediate **II**, comprising the delocalized *para*-vinylphenoxyl radical ^{a}**II** and the Co(III)-amido complex ^{b}**II** (Fig. 1c). Although this hypothesis seems tenable, HAA from O–H bonds has not been previously demonstrated with α-Co(III)-aminyl radicals **I**. Considering the potential radical addition of aminyl radicals to alkenes, it was also uncertain if α-Co(III)-aminyl radical **I** could chemoselectively react with vinylphenols **2** at the desired O–H bond through HAA rather than at the C=C bond through radical addition. Additionally, phenols are effective free radical scavengers and tend to undergo oxidative dimerization or polymerization via phenolic radicals, raising concerns about potential side reactions[35]. Furthermore, the formation of ∞-Co(III)-phenoxyl radical intermediate **II** introduces additional reactivity challenges due to the absence of a covalent linkage between the delocalized *para*-vinylphenoxyl radical ^{a}**II** and Co(III)-amido complex ^{b}**II**. If radical ^{a}**II** escapes from complex ^{b}**II**, it would terminate the desired catalytic cycle, potentially leading to radical chain reactions and other unwanted side processes. Moreover, the expected radical substitution between radical ^{a}**II** and complex ^{b}**II** via S_H2 would be kinetically demanding because concentrations of both [^{a}**II**] and [^{b}**II**] are as low as the catalyst loading. Beyond reactivity concerns, the C–N bond-forming radical substitution step would face great challenges with controlling regioselectivity. Among the four potential reacting radical centres (O1, C3, C5 and C7) in the delocalized radical intermediate ^{a}**II**, what are the determining factors that differentiate them and direct a specific radical resonance to react with Co(III)-amido complex ^{b}**II** at the nitrogen centre via S_H2 to control the regioselectivity of the amination? Would it be possible to govern the S_H2 process to occur preferentially at the remote C7 site over the nearer C3 and C5 sites without reacting at the original O1 site? This would constitute 1,7-conjugate amination with dearomatization, a transformation that has not been documented to date. In addition to the regioselectivity, the S_H2 process for C–N bond formation would also present the challenge of concurrently controlling enantioselectivity, a demanding topic that has been virtually unexplored until recently.

Catalytic asymmetric dearomative functionalization of widely available phenols represents a highly attractive approach for assembling three-dimensional molecular architectures while creating new stereogenic centres from planar phenolics[36,37]. Among different functionalization reactions, asymmetric dearomative amination of phenols is a particularly appealing strategy for the stereoselective synthesis of chiral α-tertiary amine derivatives with additional functionalities. Previous efforts have mainly considered the use of naphthols as enol nucleophiles for electrophilic amination. Using azodicarboxylates and other electrophilic aminating reagents, highly enantioselective catalytic systems have been developed for 1,3- and 1,5-conjugate amination of β- and α-naphthols, respectively, via Brønsted or Lewis acid catalysis[38–41], transition metal catalysis[42,43] and NHC catalysis[44]. In addition to the limited success in achieving asymmetric dearomative amination of non-fused phenols, 1,7-conjugate amination of 4-vinylphenols remains to be demonstrated. A survey of the literature reveals no previous reports of catalytic systems for asymmetric dearomative amination via radical pathways. This is perhaps not surprising considering the inherent propensity of phenoxyl radicals towards dimerization and polymerization together with the lack of an effective solution for controlling the regioselectivity and enantioselectivity of reactions in an extensively delocalized radical system.

Guided by the mechanistic principle of MRC, we aimed to translate these and related challenging issues into a solvable problem of catalyst development through ligand design. This would involve fine-tuning the steric, electronic and chiral environment of the versatile D_2-Por* ligand platform to develop an effective Co(II)-based metalloradical catalyst. The key strategy would be to utilize multiple non-covalent weak interactions as attractive but reversible forces to bind, position and orient the substrates and subsequent intermediates within the pocket-like ligand environment to govern the reaction pathway and the stereochemical course of the catalytic radical process. In this work, we report the successful development of a catalytic asymmetric system that is highly effective for enantioselective dearomative 1,7-conjugate amination of 4-vinylphenols with aryl azides. Through the identification of an optimal D_2-Por* as the supporting ligand, the

Co(II)-based metalloradical system can activate aryl azides at room temperature for the regioselective 1,7-amination of phenols bearing diverse *para*-substituted alkenes, affording chiral α-tertiary amino acid derivatives in high yields while creating tetrasubstituted stereocentres with high enantioselectivities. We present combined computational and experimental studies that shed light on the underlying stepwise radical mechanism of the Co(II)-catalysed 1,7-conjugate amination. To demonstrate the synthetic applications of the current catalytic radical process, we showcase a number of stereospecific transformations of the resulting α-tertiary amino acid derivatives. This study highlights the great potential of MRC for enabling asymmetric radical transformations involving increasingly complex and delocalized radical intermediates, thereby expanding the synthetic utility of radical chemistry in stereoselective molecular construction.

Results and discussion

Reaction development

To assess the feasibility of the proposed catalytic process involving delocalized 4-vinylphenoxyl radicals, we first examined the reaction of *para*-vinylphenol **2a** with 4-trifluoromethyl-2,3,5,6-tetrafluorophenyl azide (**1a**) by Co(II)-metalloradical catalysts (Fig. 2a). The selection of phenol **2a** as the substrate was based on the consideration that both *ortho*-positions are substituted with bulky ^{t}Bu groups to prevent potential homodimerization[45], while aryl azide **1a** was chosen as the aminating reagent due to its effectiveness as a metalloradicophile in Co(II)-based metalloradical systems[32,33]. It was found that the simple metalloradical catalyst [Co(**P1**)] (**P1** = tetraphenylporphyrin; Fig. 2b) was able to catalyse the reaction of vinylphenol **2a** with azide **1a**, producing the major product **3aa** in 47% yield, along with several unidentified by-products. To our delight, compound **3aa** was fully characterized as the desired dearomative 1,7-conjugate amination product. Its structure was further confirmed by X-ray crystallography, revealing the formation of *para*-quinone methide (*p*-QM) from the dearomatization of the *para*-vinylphenol and the construction of α-tertiary amino acid ester via 1,7-conjugate amination. When the first-generation chiral metalloradical catalyst [Co(**P2**)] (**P2** = ChenPhyrin; Fig. 2b)[34] was used for the reaction, the formation yield of amino esters **3aa** dramatically increased to 91% while achieving good control of enantioselectivity (71% e.e.). Excitingly, subsequent use of the analogous catalyst [Co(**P3**)] (**P3** = 3,5-di-^{t}Bu-ChenPhyrin; Fig. 2b)[34], which differs from [Co(**P2**)] by the addition of two *tert*-butyl substituents at the 3,5-positions of both 5,15-diphenyl groups without altering the chiral amide units, resulted in significant improvements in both yield (97%) and enantioselectivity (92% e.e.). However, switching to another analogous catalyst [Co(**P4**)] (**P4** = 2,6-di-MeO-ChenPhyrin; Fig. 2b)[34], which replaces the 3,5-di-*tert*-butyl substituents in [Co(**P3**)] with 2,6-di-methoxyl groups, led to dramatic decrease in both yield (20%) and enantioselectivity (70% e.e.), probably due to the more sterically encumbered ligand environment. Surprisingly, when second-generation chiral metalloradical catalyst [Co(**P5**)] (**P5** = 3,5-di-^{t}Bu-QingPhyrin; Fig. 2b) was used, only a trace amount of **3aa** (6% yield) was detected with low enantioselectivity (16% e.e.). Notably, ligand **P5** differs from ligand **P3** only by replacing one of the two distal methyl groups in **P3** with a phenyl group in the four chiral amide units. Furthermore, it was interesting to find that another second-generation chiral metalloradical catalyst [Co(**P6**)] (**P6** = 3,5-di^{t}Bu-Tao(^{t}Bu)Phyrin; Fig. 2b), which bears *tert*-butyl-ester-containing chiral amides, could restore most of the catalytic reactivity and stereoselectivity, producing **3aa** in 80% yield with 93% e.e. Together, these results demonstrate a remarkable ligand effect on the Co(II)-based metalloradical system, leading to the identification of [Co(**P3**)] as the effective catalyst for the enantioselective dearomative 1,7-conjugate amination of vinylphenol **2a** with azide **1a**. After further optimization of the reaction conditions (see Supplementary Table 1 for details), it was found that [Co(**P3**)] could effectively catalyse the transformation at room temperature in 6 h with only 1 mol% of catalyst loading, forming 1,7-conjugate amination product **3aa** in 93% isolated yield with 94% e.e. The absolute configuration of the newly generated tetrasubstituted stereogenic centre in **3aa** was established as (*R*) by X-ray crystallography.

Substrate scope

With the optimized conditions in hand, we then investigated the scope of fluoroaryl azides **1** for the catalytic dearomative 1,7-conjugate amination by [Co(**P3**)] using **2a** as the standard vinylphenol substrate (Fig. 3, entries 1–12). Like *para*-CF_3-substituted tetrafluorophenyl azide **1a**, its derivatives bearing other electron-withdrawing substituents at the *para*-position such as –CN (**1b**), $-NO_2$ (**1c**), $-SO_3Ph$ (**1d**) and $-CO_2Me$ (**1e**) could also be effectively activated by [Co(**P3**)] for dearomative 1,7-conjugate amination of the vinylphenol, generating the corresponding α-tertiary amino esters **3ba**–**3ea** bearing *p*-QM functionality in high yields with high enantioselectivities (Fig. 3, entries 2–5). In addition, tetrafluorophenyl azides with *para*-substituted halogen atoms and both electron-neutral and electron-donating groups such as –F (**1f**), –Br (**1g**), –H (**1h**) and –MeO (**1i**) could also function as excellent aminating reagents for the catalytic process, leading to high-yielding formation of amino esters **3fa**–**3ia** with high control of enantioselectivities (Fig. 3, entries 6–9). It was shown that the 1,7-conjugate amination process could be scaled up to a 2.5-mmol scale for the efficient synthesis of enantiomerically enriched amino ester **3ha** in 92% yield with 92% e.e. with only 0.5 mol% of catalyst loading, despite requiring an extended reaction time of 12 h. Furthermore, 4-tetrafluoropyridinyl azide (**1j**) could serve as a competent aminating reagent for enantioselective C–H amination of **2a**, forming the desired amino acid derivative **3ja** productively without complication from potential coordination of the pyridine unit to the cobalt centre (Fig. 3, entry 10). Additionally, [Co(**P3**)] could be similarly effective in activating difluorophenyl azides such as **1k** and **1l** for the catalytic process, generating the desired dearomative 1,7-conjugate amination products **3ka** and **3la** (Fig. 3, entries 11 and 12). It should be noted that the current Co(II)-based catalytic system is limited to aryl azides bearing fluoro substituents at both 2,6-positions. For examples, when aryl azides such as 2-bromo-3,4,6-trifluorophenyl azide, 2-bromo-4,6-difluorophenyl azide, 3,4,5-trifluorophenyl azide and 2,6-dichlorophenyl azide were used, no corresponding amination products were observed under standard conditions.

We next sought to study the scope of vinylphenols **2** for catalytic dearomative 1,7-conjugate amination by [Co(**P3**)] using azide **1h** as the common aminating reagent under the standard conditions (Fig. 3, entries 13–29). Like *para*-vinylphenol **2a** containing methyl methacrylate (Fig. 3, entry 8), *para*-vinylphenol **2b** bearing ethyl methacrylate and related derivatives with α-propyl (**2c**) and even α-octyl (**2d**) substituents at the vinyl position could effectively undergo the Co(II)-catalysed dearomative amination with azide **1h**, resulting in the production of *p*-QM-containing α-tertiary amino esters **3hb**–**3hd** bearing different α-ester and α-alkyl groups in high yields with high enantioselectivities (Fig. 3, entries 13–15). In addition to the derivatives with α-alkyl groups, *para*-vinylphenols containing various functional groups such as cyano (**2e**), ester (**2f**) and ketone (**2g**) were shown to be well tolerated and could serve as effective substrates for the catalytic process, forming the desired α-tertiary amino esters **3he**–**3hg** with the additional functionalities (Fig. 3, entries 16–18). The above results indicate that the catalytic system by [Co(**P3**)] could homolytically activate aryl azides to chemoselectively react with *para*-vinylphenols **2a**–**2g** at the desired O–H bond over the allylic C–H bonds and over the C=C bond. To further challenge the catalytic system, we designed and synthesized *para*-vinylphenols **2h**–**2j**, which contain allylic C–H bonds that are also located at the benzylic or another allylic positions. Remarkably, it was found that the Co(II)-based metalloradical system remained highly chemoselective for the enantioselective dearomative 1,7-amination of these substrates, affording the corresponding α- tertiary amino esters **3hh**–**3hj** without aminating the

https://doi.org/10.1038/s41929-025-01418-2

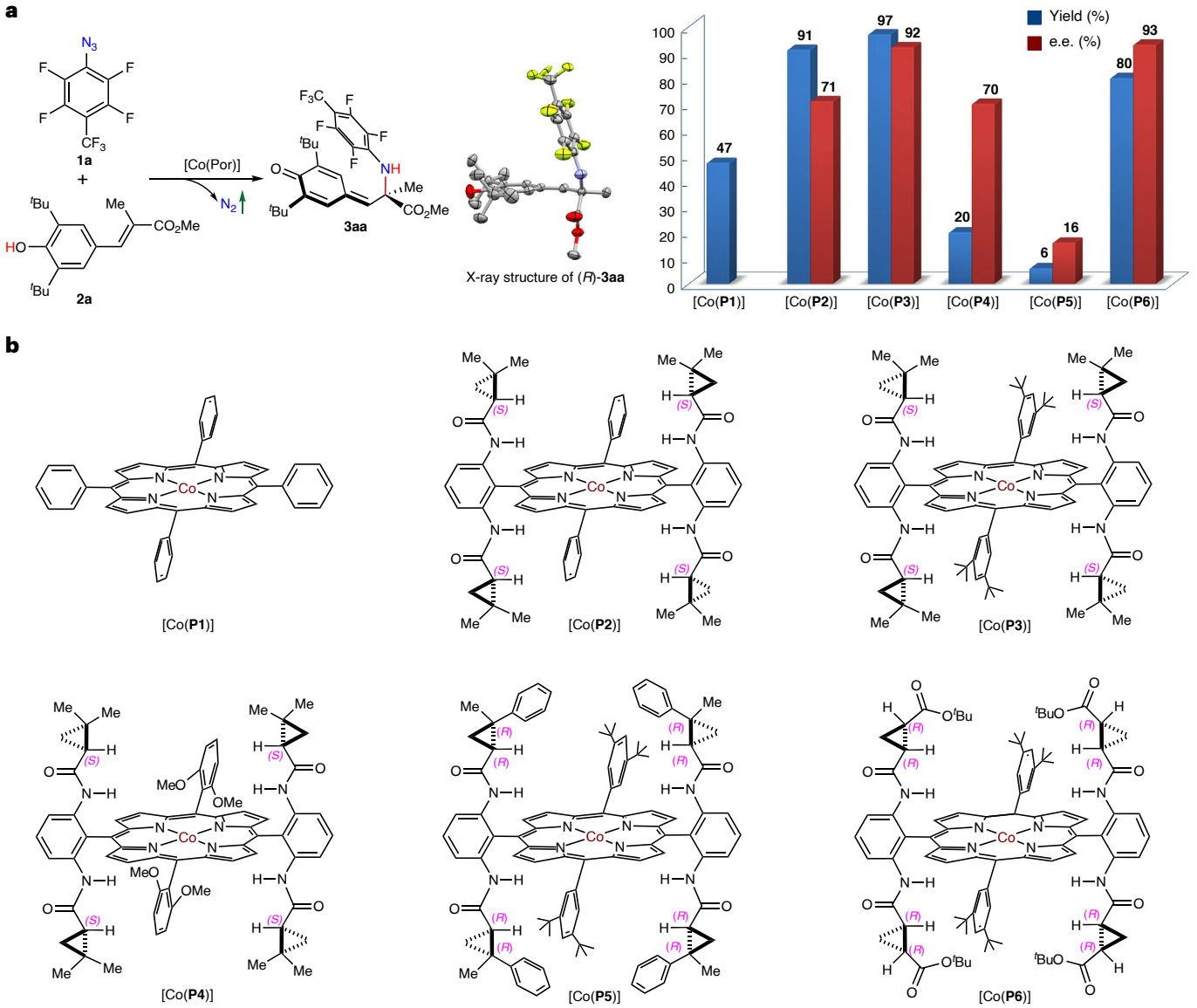

Fig. 2 | Optimization of Co(II)-based metalloradical system for dearomative amination of 4-vinylphenol with aryl azide. a, Ligand effect on [Co(Por)] (2 mol%) for dearomative amination of 4-vinylphenol **2a** (0.10 mmol) with aryl azide **1a** (0.15 mmol) in benzene (0.5 ml) at room temperature for 24 h. ^{1}H NMR yields with 1,1,2,2-tetrachloroethane as internal standard. Colour codes for X-ray structure of (*R*)-**3aa**: grey, C; red, O; blue, N; yellow, F. **b**, Structures of the Co(II)-metalloradical catalysts used in this study.

further weakened benzyl allylic and bis-allylic C–H bonds or aziridinating the additional C=C bonds (Fig. 3, entries 19–21). In addition to aminating the ester-containing *para*-vinylphenols **2a**–**2j**, [Co(**P3**)] was shown to be equally effective for the dearomative amination of *para*-vinylphenols bearing lactone (**2k**), ketone (**2l**), cyclic ketones (**2m**, **2n**) and benzocyclic ketones (**2o**, **2p**) with azide **1h**, leading to productive synthesis of enantioenriched α-tertiary amine derivatives **3hk**–**3hp** with diverse carbonyl functionalities (Fig. 3, entries 22–27). The absolute configuration of the newly generated tetrasubstituted stereogenic centre in cyclic compound **3hm** was established to be the same (*R*) configuration as that in acyclic compound **3aa** by X-ray crystallography. Moreover, *para*-vinylphenols derived from natural products, such as (−)-menthol (**2q**) and cholesterol (**2r**), could be applied as suitable substrates for [Co(**P3**)]-catalysed dearomative amination, leading to high-yielding production of natural-product-containing α-tertiary amino esters **3hq** and **3hr** with high diastereoselectivities (Fig. 3, entries 28 and 29). The results highlight the remarkable capability of the metalloradical catalyst [Co(**P3**)] to accommodate substrates of various sizes while effectively controlling stereoselectivity of the dearomative 1,7-amination process, irrespective of the existing stereogenic centres. Beyond the dearomative 1,7-conjugate amination, we further demonstrated that [Co(**P3**)] could catalyse radical 1,5- and 1,9-conjugate amination triggered by O–H HAA, as showcased for the successful generation of α-tertiary amines **3hs** and **3ht** from the dearomative amination of vinylphenols **2s** and **2t**, respectively, with azide **1h** (Fig. 3, entries 30 and 31).

Mechanistic investigations

Density function theory (DFT) calculations were conducted to examine the details of the catalytic pathways and associated energetics for asymmetric dearomative conjugate amination of vinylphenol **2a** with azide **1a** by catalyst [Co(**P3**)] (Fig. 4; see Supplementary Figs. 1–3 for details). The calculations reveal the initial formation of intermediate **A**, which results from the binding of azide **1a** to [Co(**P3**)] through the interplay of metal coordination and multiple hydrogen-bonding interactions. Subsequent spin translocation via **TS1** homolytically activates azide

https://doi.org/10.1038/s41929-025-01418-2

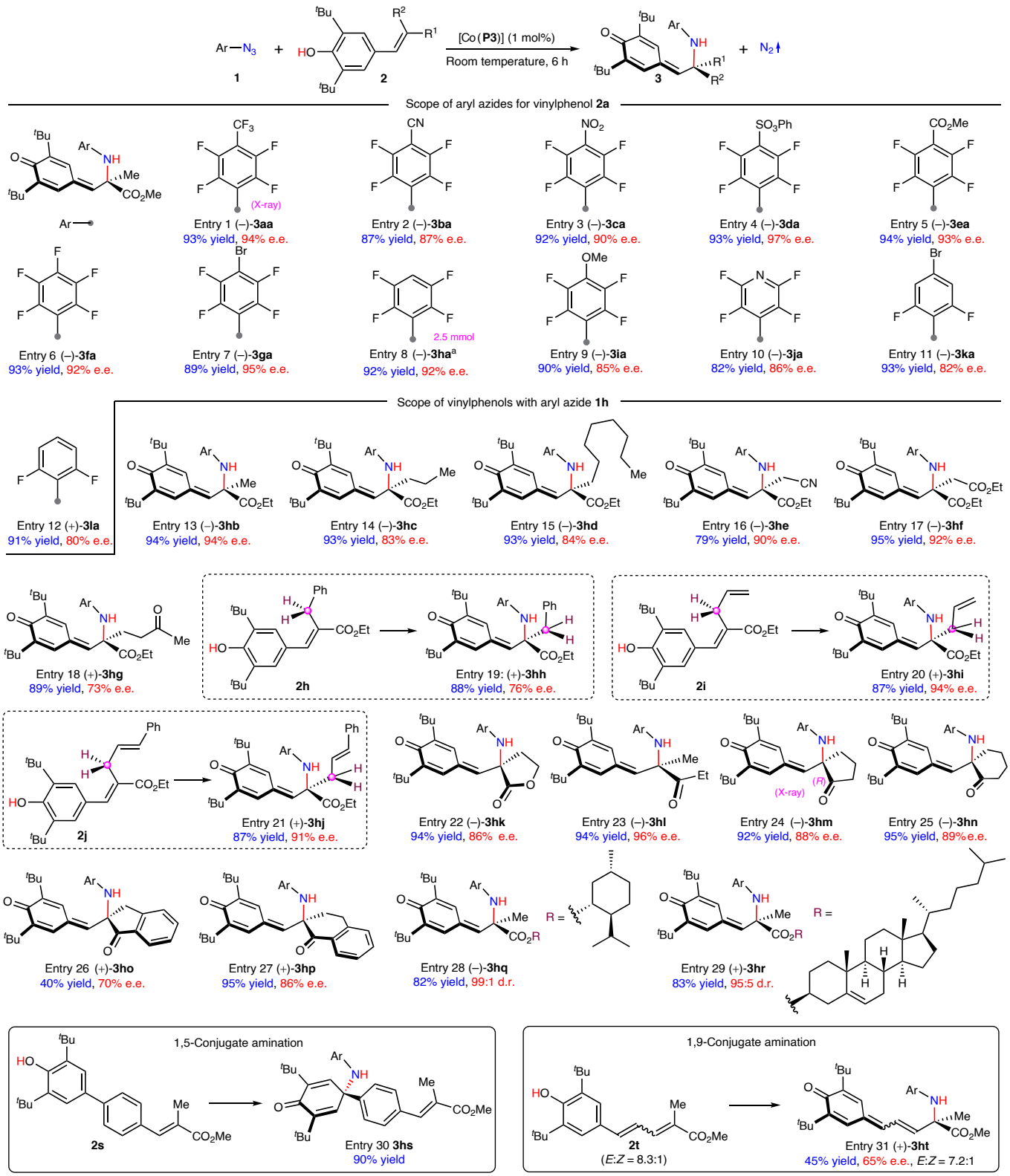

Fig. 3 | Enantioselective dearomative conjugate amination of vinylphenols with fluoroaryl azides by [Co(P3)]. Conducted with **1** (0.15 mmol) and **2** (0.10 mmol) using [Co(**P3**)] (1 mol%) in $PhCF_3$ (0.5 ml) at room temperature for 6 h. Isolated yields; e.e. determined by chiral high-performance liquid chromatography; d.r. and alkene configuration *E*:*Z* ratio determined by NMR. [a]Reaction performed on a 2.5-mmol scale using [Co(**P3**)] (0.5 mol%) at room temperature for 12 h.

1a, generating α-Co(III)-aminyl radical intermediate **B** with the elimination of dinitrogen as the by-product. This metalloradical activation, which is highly exergonic by 22.1 kcal mol^{-1}, is identified as the rate-determining step due to its relatively higher but readily accessible activation barrier ($\Delta G^{\ddagger}_{TS1}$ = 11.4 kcal mol^{-1}). As displayed in the spin plot for intermediate **B**, most of the spin density is transferred from the cobalt centre to the nitrogen atom. After binding of α-Co(III)-aminyl radical **B** with vinylphenol **2a** to form intermediate **C** through a network

https://doi.org/10.1038/s41929-025-01418-2

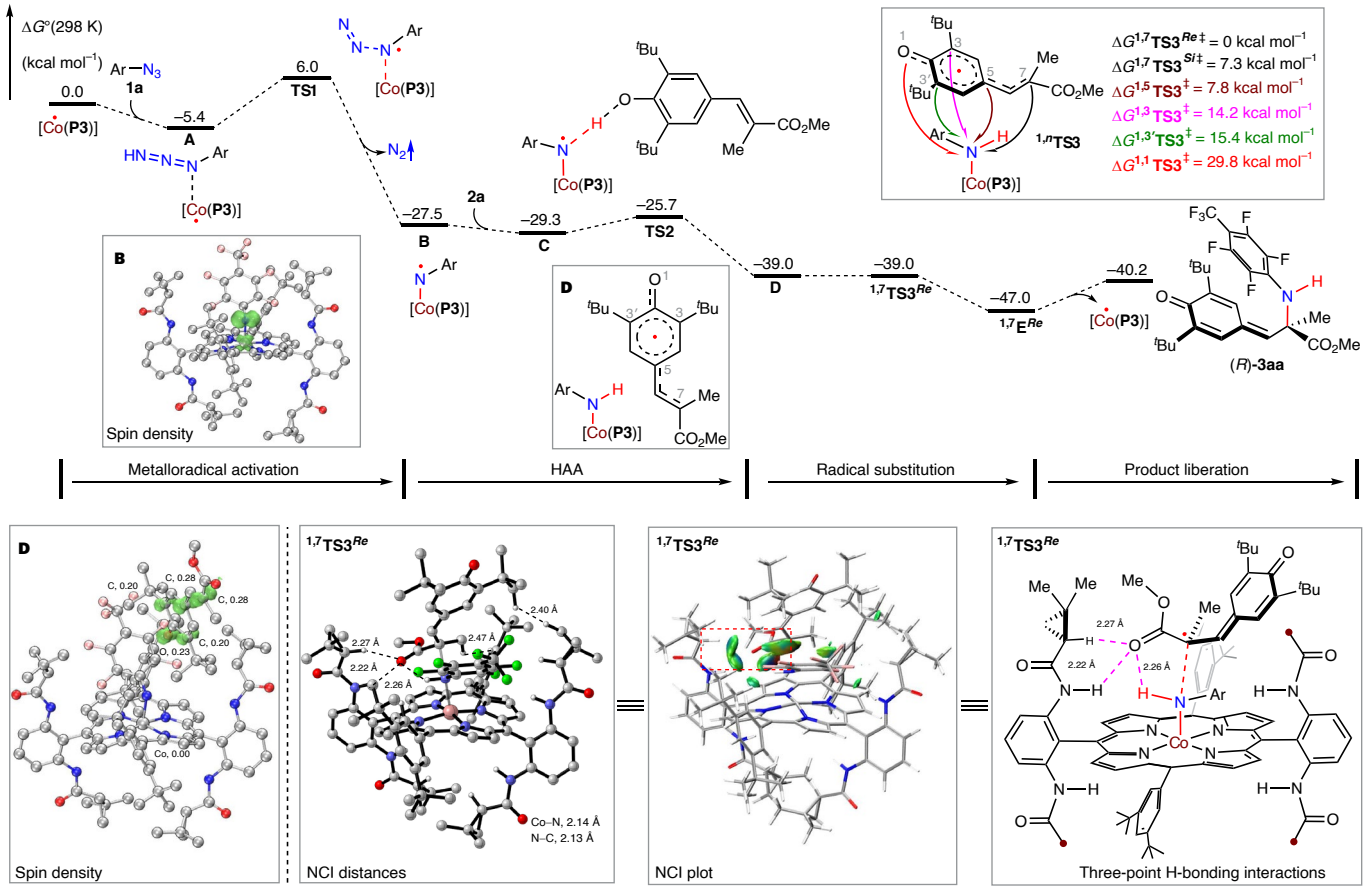

Fig. 4 | DFT study of catalytic pathways for asymmetric dearomative conjugate amination of vinylphenol 2a with azide 1a by metalloradical catalyst [Co(P3)]. The computed free energy profile ($\Delta G°$ at 298 K in kcal mol^{-1}) illustrates a stepwise radical mechanism, including (1) metalloradical activation of azide **1a** by [Co(**P3**)], proceeding through intermediate **A** to generate α-Co(III)-aminyl radical intermediate **B** via transition state **TS1**; (2) HAA from the O–H bond of vinylphenol **2a** by intermediate **B**, passing through intermediate **C** to afford ∞-Co(III)-amido phenoxyl radical intermediate **D** via transition state **TS2**; (3) radical substitution within intermediate **D**, involving the phenoxyl radical and the Co(III)-amido complex to form intermediate ^{1,7}**E**^{Re} via transition state ^{1,7}**TS3**^{Re}; and (4) product liberation from intermediate ^{1,7}**E**^{Re} to release the final α-tertiary amino ester (*R*)-**3aa**. Insets: relative Gibbs free energy barriers ($\Delta G^{\ddagger}$) for competing radical substitution pathways at different positions (upper right); spin density plots for intermediates **B** and **D**, respectively (middle and bottom left); NCI plots and schematic illustration of transition state structure ^{1,7}**TS3**^{Re} (bottom centre and right). All calculations were carried out at the SMD(benzene)-BP86-D3(BJ)/def2TZVP//BP86/def2SVP level of theory. Colour codes for the structures: grey, C; red, O; blue, N; green, F.

of non-covalent interactions (NCIs), the O–H group of the vinylphenol is positioned in close proximity to the nitrogen-centred radical, allowing for a kinetically facile and thermodynamically favourable HAA via **TS2** ($\Delta G^{\ddagger}_{\mathbf{TS2}}$ = 3.6 kcal mol^{-1}; $\Delta G°$ = −9.7 kcal mol^{-1}). This step leads to the generation of ∞-Co(III)-amido phenoxyl radical intermediate **D**. As shown in the spin plot for intermediate **D**, the spin density is extensively delocalized across the large π-conjugate system of the *para*-vinylphenoxyl radical unit. According to the DFT calculations, the final step of radical substitution at the α-position of the ester functionality via ^{1,7}**TS3**^{Re}, which is exergonic by 8.0 kcal mol^{-1}, is found to be nearly barrierless, resulting in the formation of 1,7-amination product (*R*)-**3aa**, which remains bound to [Co(**P3**)] as intermediate ^{1,7}**E**^{Re} before dissociating as free amino ester **3aa** while regenerating metalloradical catalyst [Co(**P3**)]. The activation barrier ($\Delta G^{\ddagger}_{1,7_{\mathbf{TS3}Si}}$) associated with the formation of the minor enantiomer (*S*)-**3aa** is found to be 7.3 kcal mol^{-1} higher than that for the preferred formation of (*R*)-**3aa**. Although the calculated energy difference ($\Delta\Delta G^{\ddagger}$) quantitatively overestimated the experimentally observed enantioselectivity, this significant energy gap clearly rationalizes the experimental preference for the *Re*-face substitution. Further DFT calculations show that the activation barriers ($\Delta G^{\ddagger}_{1,\mathbf{n}_{\mathbf{TS3}Si}}$) associated with the transition states ^{1,n}**TS3** of radical substitution at other possible sites are significantly higher than $\Delta G^{\ddagger}_{1,7_{\mathbf{TS3}Re}}$ ($\Delta G^{\ddagger}_{1,1_{\mathbf{TS3}}}$ [= 29.8 kcal mol^{-1}; $\Delta G^{\ddagger}_{1,3'_{\mathbf{TS3}}}$ = 15.4 kcal mol^{-1}; $\Delta G^{\ddagger}_{1,3_{\mathbf{TS3}}}$ = 14.2 kcal mol^{-1}; $\Delta G^{\ddagger}_{1,5_{\mathbf{TS3}}}$ = 7.8 kcal mol^{-1}). These computational results align with the experimentally observed regioselectivity for exclusive 1,7-amination without complications from potential 1,1-, 1,3- and 1,5-amination reactions. As illustrated by the NCI plots of the DFT-optimized transition state structure ^{1,7}**TS3**^{Re}, it is the multiple attractive NCIs within the pocket of the catalyst that together hold the delocalized *para*-vinylphenoxyl radical in the proper orientation and conformation. This precise arrangement positions the C-7 site of the *para*-vinylphenoxyl radical in close proximity to the nitrogen centre of the Co(III)-amido complex, facilitating the highly regioselective C–N bond formation while also enabling effective asymmetry induction. Among different types of NCIs in the transition state ^{1,7}**TS3**^{Re}, it is worth highlighting the unique three-point hydrogen-bonding interactions between the C=O group of the *para*-vinylphenoxyl radical and the N–H, C–H and N–H groups in the Co(III)-amido complex, which is supported by D_2-symmmetic chiral amidoporphyrin **P3** (Fig. 4). These specific interactions play a crucial role in stabilizing the transition state, guiding regioselectivity and ensuring enantioselectivity in the catalytic process.

In addition to the computational studies, significant efforts were devoted to detecting and probing the radical intermediates involved in the stepwise radical mechanism of the Co(II)-catalysed

https://doi.org/10.1038/s41929-025-01418-2

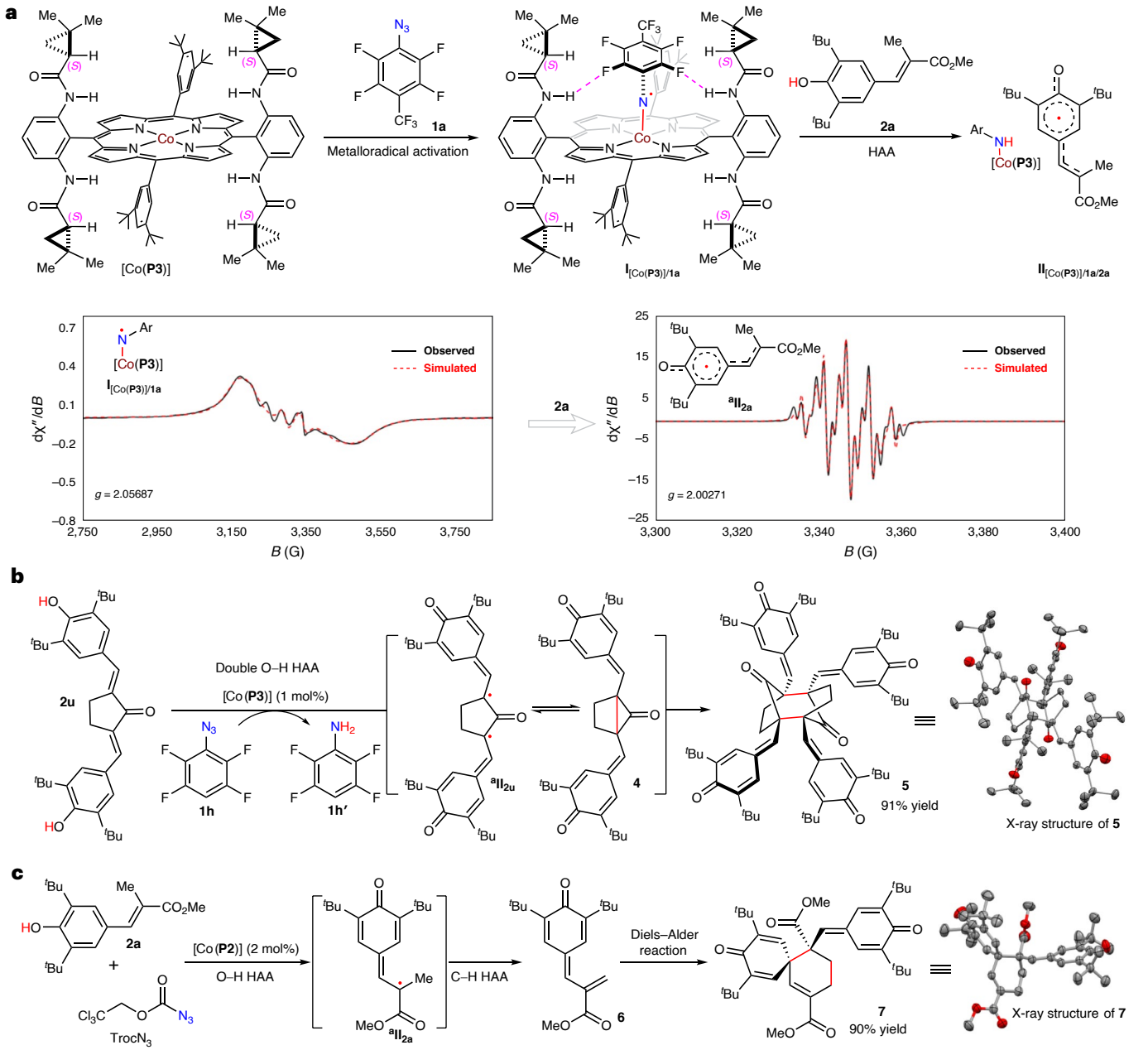

Fig. 5 | Mechanistic studies on the Co(II)-based metalloradical system for 1,7-conjugate amination of vinylphenols with azides. a, Detection of α-Co(III)-aminyl radical and ∞-Co(III)-amido vinylphenoxyl radical intermediates by EPR. **b**, Probing of delocalized *para*-vinylphenoxyl radical intermediate through formation and homodimerization of bis-allylic oxyallyl biradical. **c**, Probing of delocalized *para*-vinylphenoxyl radical intermediate through formation and Diels–Alder dimerization of conjugate diene.

1,7-conjugate amination (Fig. 5). To directly detect the α-Co(III)-aminyl radical intermediate **I**, an isotropic X-band electron paramagnetic resonance (EPR) spectrum was recorded at ambient temperature for the reaction mixture of [Co(**P3**)] with azide **1a** in benzene without the vinylphenol substrate (Fig. 5a). The spectrum displays distinct signals characteristic of α-Co(III)-aminyl radicals[32]. Both the isotopic *g*-value of 2.05687 and the hyperfine couplings of the observed peaks are consistent with the generation of α-Co(III)-aminyl radical $\mathbf{I}_{[Co(P3)]/1a}$ from metalloradical activation of azide **1a** by [Co(**P3**)]. Upon adding vinylphenol **2a** into the reaction mixture, the relatively weak and broad signals associated with $\mathbf{I}_{[Co(P3)]/1a}$ disappeared and were replaced by strong and sharp signals. The new EPR signals, with an isotopic *g*-value of 2.00271, indicate the generation of the *para*-vinylphenoxyl radical $^{a}\mathbf{II}_{2a}$ as part of ∞-Co(III)-amido vinylphenoxyl radical intermediate $\mathbf{II}_{[Co(P3)]/1a/2a}$, along with Co(III)-amido complex $^{b}\mathbf{II}_{[Co(P3)]/1a}$, through HAA from the O–H bond of vinylphenol **2a** by the initially generated α-Co(III)-aminyl radical $\mathbf{I}_{[Co(P3)]/1a}$. Consistent with the spin delocalization in vinylphenoxyl radical $^{a}\mathbf{II}_{2a}$, the well-defined EPR spectrum could be nicely simulated by taking into account its various resonance structures (see Supplementary Figs. 4 and 5 for details). To further probe the O–H HAA step and the resulting delocalized radical intermediate, cyclopentanone-based bis-vinylphenol **2u** was synthesized and used as the substrate in the catalytic reaction with azide **1h** by [Co(**P3**)] (Fig. 5b). It was anticipated that the ethano-bridged bis-allylic oxyallyl biradical $^{a}\mathbf{II}_{2u}$ would form via double HAA from the two O–H bonds of substrate **2u** by the initially generated α-Co(III)-aminyl radical $\mathbf{I}_{[Co(P3)]/1h}$. Instead

https://doi.org/10.1038/s41929-025-01418-2

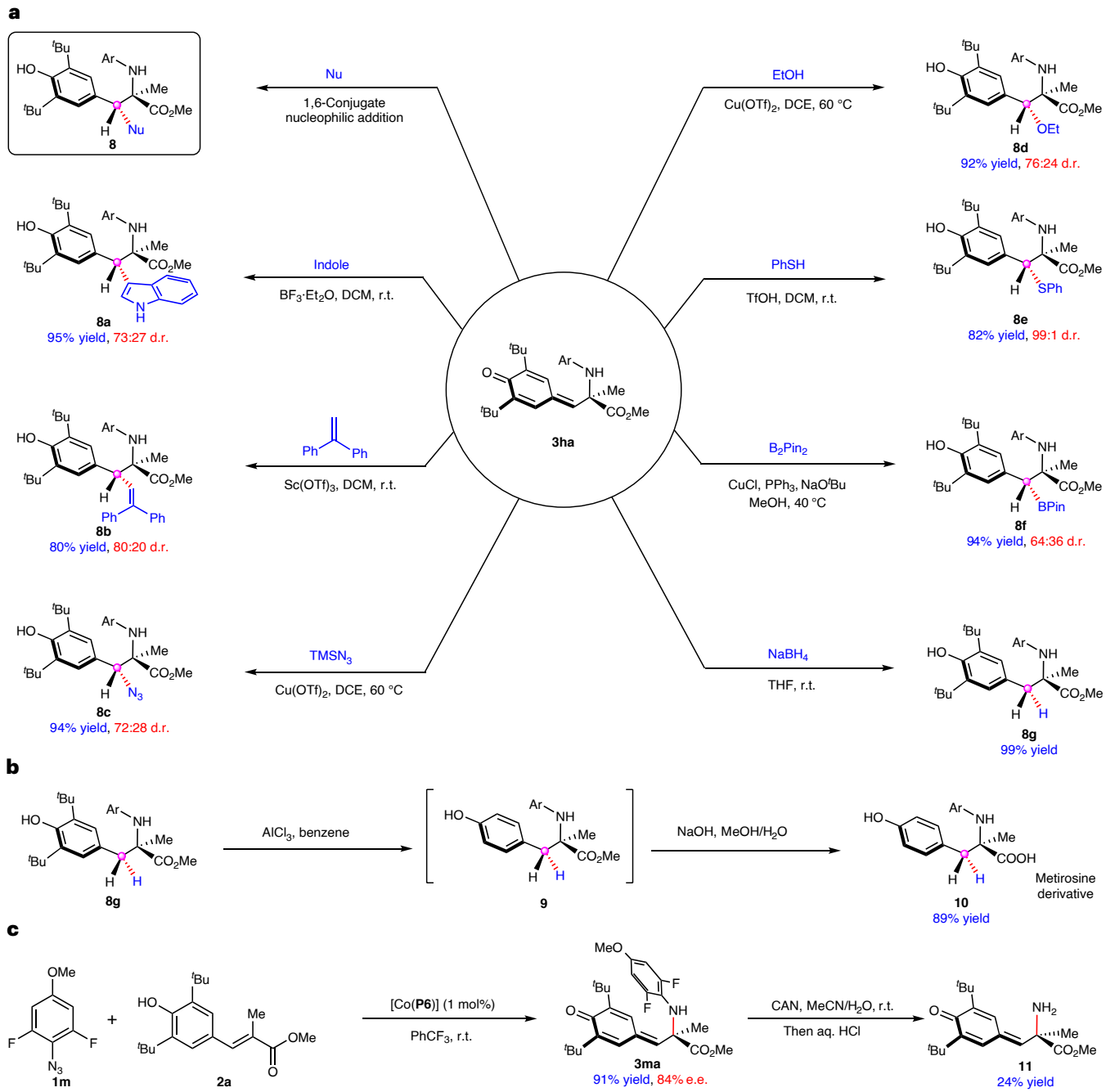

Fig. 6 | Synthetic applications of resulting α-amino acid derivatives from 1,7-conjugate amination of vinylphenols with azides. a, Further transformations via 1,6-conjugate addition of *p*-QM functionality with diverse nucleophiles. DCM, dichloromethane; DCE, 1,2-dichloroethane; THF, tetrahydrofuran; CAN, ceric ammonium nitrate. **b**, Synthesis of α-methyltyrosine derivative through de-*tert*-butylation and ester hydrolysis. **c**, Synthesis of α-tertiary primary amino acid derivative by deprotection of the *N*-aryl group.

of undergoing radical substitution for C–N bond formation, biradical $^{a}\mathbf{II}_{2u}$ was expected to proceed via intramolecular radical recombination, yielding the corresponding ethano-bridged cyclopropanone **4** through C–C bond formation[46]. Although no amination product was observed, the catalytic reaction resulted in the isolation of product **5** in 91% yield, along with tetrafluoroaniline **1h′** as the by-product (Fig. 5b). X-ray crystallography confirmed that compound **5** is a tricyclic diketone bearing four *p*-QMs, which was evidently formed through the dimerization of biradical $^{a}\mathbf{II}_{2u}$. Interestingly, when compound **5** was dissolved in benzene at room temperature, notable EPR signals at the isotopic *g*-value of 2.00489 were detected, indicating the generation of biradical $^{a}\mathbf{II}_{2u}$ from homolytic cleavage of the two elongated weak C(4°)–C(4°) bonds (see Supplementary Fig. 6 for details). In a separate experiment to probe the stepwise radical mechanism, 2,2,2-trichloroethoxycarbonyl azide ($TrocN_3$) was used in place of aryl azides in the catalytic reaction of vinylphenol **2a** with [Co(**P2**)] as the catalyst (Fig. 5c). Rather than forming the corresponding amination product, the catalytic reaction led to the isolation of compound **7** in 90% yield. X-ray crystallography revealed that compound **7** possesses a spiro[6.6]bicyclic structure, featuring an additional quaternary carbon bonded to the shared quaternary carbon. Evidently, compound **7** is a dimer of the dehydrogenation compound **6** resulted from a Diels–Alder reaction. Compound **6** probably originated from secondary HAA from the substantially weakened α-C–H bond of the initially generated *para*-vinylphenoxyl radical $^{a}\mathbf{II}_{2a}$, a competitive

process that became favoured over the radical substitution for C–N bond formation. Analogous to $TrocN_3$, arylsulfonyl azides were also found to exclusively promote the dehydrogenation pathway under the standard reaction condition, completely suppressing the formation of amination products.

Synthetic applications

In addition to being a common structural motif in many biologically active natural products, *p*-QMs are known for their diverse chemical reactivities, including their effectiveness as Michael acceptors in conjugate addition reactions with nucleophiles[47]. To demonstrate the synthetic applications of the *p*-QM-containing α-tertiary amino esters produced from the Co(II)-catalysed 1,7-conjugate amination, a series of further synthetic transformations were performed using **3ha** as a model compound (Fig. 6). It was shown that α-tertiary amino ester **3ha** could serve as a versatile building block to access highly functionalized chiral amino esters **8** while creating an additional stereogenic centre adjacent to the original one through 1,6-conjugate addition reactions with a variety of nucleophiles (Fig. 6a). For example, electron-rich aromatic compounds such as indole could act as a carbon-based nucleophile to react with **3ha** in the presence of $BF_3{\cdot}Et_2O$ as catalyst, affording β-aryl-α-tertiary amino ester **8a** in excellent yield, although with moderate diastereoselectivity. Additionally, **3ha** could undergo $Sc(OTf)_3$-catalysed 1,6-conjugate addition with 1,1-diphenylethylene, forming β-vinyl-α-tertiary amino ester **8b** in high yield with good diastereoselectivity. Under $Cu(OTf)_2$ catalysis, **3ha** could also react with both nitrogen-based nucleophile $TMSN_3$ and oxygen-based nucleophile ethanol, leading to high-yielding syntheses of β-azido-α-tertiary amino ester **8c** and β-ethoxy-α-tertiary amino ester **8d**, respectively, albeit with moderate diastereoselectivities. Similarly, triflic acid-catalysed 1,6-conjugate addition of **3ha** with sulfur-based nucleophile PhSH produced β-thiol-α-tertiary amino ester **8e** in high yield with excellent diastereoselectivity for the newly created adjacent stereogenic centre. Furthermore, copper-catalysed 1,6-conjugate addition of **3ha** with $B_2(pin)_2$ provided an attractive route for the synthesis of β-boryl-α-tertiary amino ester **8f** in high yield, albeit with moderate diastereoselectivity. Moreover, reduction of **3ha** using $NaBH_4$ resulted in the formation α-tertiary amino ester **8g** in quantitative yield. In essence, the combination of the 1,6-conjugate addition with the Co(II)-catalysed 1,7-conjugate amination enables difunctionalization of the trisubstituted alkene units of the starting vinylphenols **2**, facilitating the stereoselective synthesis of highly functionalized chiral amino esters **8** with the creation of two adjacent stereogenic centres. As a demonstration for the synthesis of α-methyltyrosine derivative, it was shown that the two ortho-*tert*-butyl groups in the phenol unit of the α-tertiary amino ester **8g** could be readily removed through $AlCl_3$-mediated de-*tert*-butylation, yielding α-methyltyrosine methyl ester **9** (Fig. 6b). Without further purification, ester **9** was directly subjected to hydrolysis, affording metirosine derivative **10**, an inhibitor of the tyrosine hydroxylase enzyme, in 89% overall yield from the starting material **8g**. In a separate demonstration for the synthesis of α-tertiary primary amino acid derivative (Fig. 6c), *N*-aryl amino ester **3ma**, which was synthesized from [Co(**P6**)]-catalysed 1,7-conjugate amination of vinylphenol **2a** with 2,6-difluoro-4-methyoxyphenyl azide (**1m**) in 91% yield with 84% e.e., was shown to undergo ceric ammonium nitrate oxidation followed by in situ acid hydrolysis, furnishing the unprotected α-tertiary primary amino ester **11**. However, the low yield of this de-N-arylation process suggests that further optimization is needed.

Conclusion

We have successfully developed the first catalytic system via Co(II)-based MRC that is highly effective for enantioselective radical dearomative conjugate amination. Facilitated by an optimal D_2-symmetric chiral amidoporphyrin ligand, the Co(II)-based metalloradical system can homolytically activate aryl azides for dearomative 1,7-conjugate amination of *para*-vinylphenols with concurrent control of chemoselectivity, regioselectivity and enantioselectivity. This Co(II)-catalysed radical amination, which operates at room temperature with low catalyst loading without the need for oxidants or other additives, provides an attractive methodology for the stereoselective synthesis of valuable chiral α-tertiary amino acid derivatives, while generating N_2 as the sole by-product. We have demonstrated that the resulting amino acid esters, bearing *p*-QM functionality, can undergo 1,6-conjugate addition with various nucleophiles, enabling the stereoselective synthesis of highly functionalized α-tertiary amino derivatives bearing two adjacent stereogenic centres. Unlike Co(II)-based C–H amination, this dearomative conjugate amination proceeds through an extensively delocalized 4-vinylphenoxyl radical intermediate, formed via uncommon HAA from O–H bonds of phenols by the initially generated α-Co(III)-aminyl radicals, followed by regioselective radical substitution to achieve remote 1,7-amination. The success in concurrently controlling multiple selectivities in this challenging radical process is attributed to the catalyst innovation by leveraging a network of non-covalent weak interactions within the pocket-like environment of the D_2-symmetric chiral amidoporphyrin ligand platform. Along with our preliminary demonstration of dearomative 1,5- and 1,9-conjugate amination, we anticipate that this work will inspire further research endeavours aimed at exploring the untapped synthetic potential of extensively delocalized radical systems.

Methods

In a general procedure for Co(II)-catalysed enantioselective dearomative conjugate amination, an oven-dried Schlenk tube was charged with Co(II)-metalloradical catalyst [Co(**P3**)] (1 mol%, 1.4 mg) and vinylphenol **2** (0.10 mmol, 1.0 equiv.). The Schlenk tube was evacuated and backfilled with nitrogen three times. After replacing the Teflon screw cap with a rubber septum, aryl azide **1** (0.15 mmol, 1.5 equiv.) and trifluorotoluene (0.5 ml) were added via a gas-tight syringe. The resulting mixture was then purged with nitrogen for 30 s, resealed with the Teflon screw cap and stirred at room temperature for 6 h. Upon completion, the reaction mixture was concentrated by rotary evaporation under reduced pressure. The residue was subject to purification by flash chromatography on silica gel to afford the pure dearomative amination product **3**.

Data availability

Crystallographic data for the structures reported in this article have been deposited at the Cambridge Crystallographic Data Centre, under deposition numbers CCDC 2411816 (**3aa**), 2411818 (**3hm**), 2411819 (**5**) and 2411820 (**7**). Copies of the data can be obtained free of charge via https://www.ccdc.cam.ac.uk/structures/. All other data that support the findings of this study, which include experimental procedures and compound characterization, are available within the paper and its Supplementary Information. Data are available from the corresponding author upon request.

References

1. Chatgilialoglu, C. & Studer, A. *Encyclopedia of Radicals in Chemistry, Biology and Materials* (Wiley, 2012).
2. Mondal, S. et al. Enantioselective radical reactions using chiral catalysts. *Chem. Rev.* **122**, 5842–5976 (2022).
3. Chen, C. & Fu, G. C. Copper-catalysed enantioconvergent alkylation of oxygen nucleophiles. *Nature* **618**, 301–307 (2023).
4. Chen, C., Peters, J. C. & Fu, G. C. Photoinduced copper-catalysed asymmetric amidation via ligand cooperativity. *Nature* **596**, 250–256 (2021).
5. Chen, J.-J. et al. Enantioconvergent Cu-catalysed N-alkylation of aliphatic amines. *Nature* **618**, 294–300 (2023).
6. Gu, Q.-S., Li, Z.-L. & Liu, X.-Y. Copper(I)-catalyzed asymmetric reactions involving radicals. *Acc. Chem. Res.* **53**, 170–181 (2020).

7. Proctor, R. S. J., Colgan, A. C. & Phipps, R. J. Exploiting attractive non-covalent interactions for the enantioselective catalysis of reactions involving radical intermediates. *Nat. Chem.* **12**, 990–1004 (2020).
8. Proctor, R. S. J., Davis, H. J. & Phipps, R. J. Catalytic enantioselective minisci-type addition to heteroarenes. *Science* **360**, 419 (2018).
9. Zhang, Z., Chen, P. & Liu, G. Copper-catalyzed radical relay in C(sp^3)-H functionalization. *Chem. Soc. Rev.* **51**, 1640–1658 (2022).
10. Li, J. et al. Site-specific allylic C–H bond functionalization with a copper-bound N-centred radical. *Nature* **574**, 516–521 (2019).
11. Kern, N., Plesniak, M. P., McDouall, J. J. W. & Procter, D. J. Enantioselective cyclizations and cyclization cascades of samarium ketyl radicals. *Nat. Chem.* **9**, 1198–1204 (2017).
12. Lee, W.-C. C. & Zhang, X. P. Metalloradical catalysis: general approach for controlling reactivity and selectivity of homolytic radical reactions. *Angew. Chem. Int. Ed.* **63**, e202320243 (2024).
13. RajanBabu, T. V. & Nugent, W. A. Selective generation of free radicals from epoxides using a transition-metal radical. A powerful new tool for organic synthesis. *J. Am. Chem. Soc.* **116**, 986–997 (1994).
14. Nugent, W. A. & RajanBabu, T. V. Transition-metal-centered radicals in organic synthesis. Titanium(III)-induced cyclization of epoxy olefins. *J. Am. Chem. Soc.* **110**, 8561–8562 (1988).
15. Zhang, Z. et al. A chiral titanocene complex as regiodivergent photoredox catalyst: synthetic scope and mechanism of catalyst generation. *J. Am. Chem. Soc.* **145**, 26667–26677 (2023).
16. Yao, C., Dahmen, T., Gansäuer, A. & Norton, J. Anti-Markovnikov alcohols via epoxide hydrogenation through cooperative catalysis. *Science* **364**, 764–767 (2019).
17. Ye, K.-Y., McCallum, T. & Lin, S. Bimetallic radical redox-relay catalysis for the isomerization of epoxides to allylic alcohols. *J. Am. Chem. Soc.* **141**, 9548–9554 (2019).
18. Hao, W. et al. Radical redox-relay catalysis: formal [3+2] cycloaddition of *N*-acylaziridines and alkenes. *J. Am. Chem. Soc.* **139**, 12141–12144 (2017).
19. Agasti, S. et al. A catalytic alkene insertion approach to bicyclo[2.1.1]hexane nioisosteres. *Nat. Chem.* **15**, 535–541 (2023).
20. Huang, H.-M., McDouall, J. J. W. & Procter, D. J. SmI_2-catalysed cyclization cascades by radical relay. *Nat. Catal.* **2**, 211–218 (2019).
21. Xu, H., Wang, D.-S., Zhu, Z., Deb, A. & Zhang, X. P. New mode of asymmetric induction for enantioselective radical N-heterobicyclization via kinetically stable chiral radical center. *Chem* **10**, 283–298 (2024).
22. Lee, W.-C. C., Wang, D.-S., Zhu, Y. & Zhang, X. P. Iron(III)-based metalloradical catalysis for asymmetric cyclopropanation via a stepwise radical mechanism. *Nat. Chem.* **15**, 1569–1580 (2023).
23. Epping, R. F. J., Hoeksma, M. M., Bobylev, E. O., Mathew, S. & de Bruin, B. Cobalt(II)-tetraphenylporphyrin-catalysed carbene transfer from acceptor–acceptor iodonium ylides via *N*-enolate–carbene radicals. *Nat. Chem.* **14**, 550–557 (2022).
24. Zhou, M. et al. Catalytic synthesis of 1H-2-benzoxocins: cobalt(III)-carbene radical approach to 8-membered heterocyclic enol ethers. *J. Am. Chem. Soc.* **143**, 20501–20512 (2021).
25. Das, S., Ehlers, A. W., Patra, S., de Bruin, B. & Chattopadhyay, B. Iron-catalyzed intermolecular C–N cross-coupling reactions via radical activation mechanism. *J. Am. Chem. Soc.* **145**, 14599–14607 (2023).
26. Khatua, H. et al. Iron-catalyzed intermolecular amination of benzylic C(sp^3)–H bonds. *J. Am. Chem. Soc.* **144**, 21858–21866 (2022).
27. Roy, S. et al. Iron-catalyzed radical activation mechanism for denitrogenative rearrangement over C(sp^3)–H amination. *Angew. Chem. Int. Ed.* **60**, 8772–8780 (2021).
28. Roy, S., Khatua, H., Das, S. K. & Chattopadhyay, B. Iron(II)-based metalloradical activation: switch from traditional click chemistry to denitrogenative annulation. *Angew. Chem. Int. Ed.* **58**, 11439–11443 (2019).
29. Roy, S., Das, S. K. & Chattopadhyay, B. Cobalt(II)-based metalloradical activation of 2-(diazomethyl)pyridines for radical transannulation and cyclopropanation. *Angew. Chem. Int. Ed.* **57**, 2238–2243 (2018).
30. Mendel, M. et al. Dynamic stereomutation of vinylcyclopropanes with metalloradicals. *Nature* **631**, 80–86 (2024).
31. Kapat, A., Sperger, T., Guven, S. & Schoenebeck, F. *E*-Olefins through intramolecular radical relocation. *Science* **363**, 391–396 (2019).
32. Jin, L.-M., Xu, P., Xie, J. & Zhang, X. P. Enantioselective intermolecular radical C–H amination. *J. Am. Chem. Soc.* **142**, 20828–20836 (2020).
33. Xu, P., Xie, J., Wang, D.-S. & Zhang, X. P. Metalloradical approach for concurrent control in intermolecular radical allylic C–H amination. *Nat. Chem.* **15**, 498–507 (2023).
34. Chen, Y., Fields, K. B. & Zhang, X. P. Bromoporphyrins as versatile synthons for modular construction of chiral porphyrins: cobalt-catalyzed highly enantioselective and diastereoselective cyclopropanation. *J. Am. Chem. Soc.* **126**, 14718–14719 (2004).
35. Kobayashi, S. & Higashimura, H. Oxidative polymerization of phenols revisited. *Prog. Polym. Sci.* **28**, 1015–1048 (2003).
36. Zhuo, C.-X., Zhang, W. & You, S.-L. Catalytic asymmetric dearomatization reactions. *Angew. Chem. Int. Ed.* **51**, 12662–12686 (2012).
37. Wu, W.-T., Zhang, L. & You, S.-L. Catalytic asymmetric dearomatization (CADA) reactions of phenol and aniline derivatives. *Chem. Soc. Rev.* **45**, 1570–1580 (2016).
38. Wang, S.-G., Yin, Q., Zhuo, C.-X. & You, S.-L. Asymmetric dearomatization of β-naphthols through an amination reaction catalyzed by a chiral phosphoric acid. *Angew. Chem. Int. Ed.* **54**, 647–650 (2015).
39. Xia, Z.-L., Zheng, C., Xu, R.-Q. & You, S.-L. Chiral phosphoric acid catalyzed aminative dearomatization of α-naphthols/Michael addition sequence. *Nat. Commun.* **10**, 3150 (2019).
40. Nan, J. et al. Direct asymmetric dearomatization of 2-naphthols by scandium-catalyzed electrophilic amination. *Angew. Chem. Int. Ed.* **54**, 2356–2360 (2015).
41. Lian, X., Lin, L., Wang, G., Liu, X. & Feng, X. Chiral *N*,*N*'-dioxide-scandium(III)-catalyzed asymmetric dearomatization of 2-naphthols through an amination reaction. *Chem. Eur. J.* **21**, 17453–17458 (2015).
42. Lee, E., Hwang, Y., Kim, Y. B., Kim, D. & Chang, S. Enantioselective access to spirolactams via nitrenoid transfer enabled by enhanced noncovalent interactions. *J. Am. Chem. Soc.* **143**, 6363–6369 (2021).
43. Wang, C.-J. et al. Enantioselective copper-catalyzed electrophilic dearomative azidation of β-naphthols. *Org. Lett.* **21**, 7315–7319 (2019).
44. Maji, U., Mondal, B. D. & Guin, J. Asymmetric aminative dearomatization of 2-naphthols via non-covalent N-heterocyclic carbene catalysis. *Org. Lett.* **25**, 2323–2327 (2023).
45. Keylor, M. H. et al. Synthesis of resveratrol tetramers via a stereo-convergent radical equilibrium. *Science* **354**, 1260–1265 (2016).
46. Masters, A. P., Parvez, M., Sorensen, T. S. & Sun, F. Attempted generation of an observable ethano-bridged (cyclopentyl) oxyallyl. The pericyclic nature of an oxyallyl–oxyallyl dimerization reaction. *J. Am. Chem. Soc.* **116**, 2804–2811 (1994).
47. Lima, C. G. S. et al. *para*-Quinone methides as acceptors in 1,6-nucleophilic conjugate addition reactions for the synthesis of structurally diverse molecules. *Eur. J. Org. Chem.* **2020**, 2650–2692 (2020).

Acknowledgements
We are grateful for financial support from the NIH (R35-GM156311, R01-GM132471 and R01-GM102554 to X.P.Z.) and in part by the NSF (CHE-2154885 to X.P.Z.). Z.Z. was supported by a LaMattina Graduate Fellowship. We are also grateful for financial support from the NIH (S10-OD026910) and the NSF (CHE-2117246) for the purchase of NMR spectrometers at the Magnetic Resonance Center of Boston College and by the NIH (S10-OD030360) for the purchase of an X-ray single-crystal diffractometer at the X-ray Crystallography Center of Boston College.

Author contributions
X.P.Z. conceived of the work and directed the project. P.X. conducted the experiments. D.-S.W. conducted DFT calculations. Z.Z. assisted the project. P.X. and X.P.Z. designed the experiments. P.X. and X.P.Z. wrote the paper.

Competing interests
The authors declare no competing interests.

Additional information
Supplementary information The online version contains supplementary material available at https://doi.org/10.1038/s41929-025-01418-2.

Correspondence and requests for materials should be addressed to X. Peter Zhang.

Peer review information *Nature Catalysis* thanks Malek Nechab, Ángel Rentería-Gómez and the other, anonymous, reviewer(s) for their contribution to the peer review of this work.